

Understanding ULX Nebulae in the Framework of Supercritical Accretion

P. Abolmasov

Sternberg Astronomical Institute, Moscow State University Moscow, Russia 119992;
Email: pavel.abolmasov@yahoo.co.uk

Abstract

For a long time, the well-known supercritically accreting binary SS433 is being proposed as a prototype for a class of hypothetical bright X-ray sources that may be identified with the so-called Ultraluminous X-ray sources (ULXs) in nearby galaxies or at least with part of them. Like SS433, these objects should be associated with optical nebulae, powered by both radiation of the central source and its wind or jet activity. Indeed, around many ULXs, bright optical nebulae (ULX Nebulae, ULXNe) are found. Here, we use SS433 as a prototype for the power source creating the nebulae around ULXs. Though many factors are important such as the structure of the host star-forming region and the possible supernova remnant formed together with the accreting compact object, we show that most of the properties of ULXNe may be explained by an SS433-like system evolving for up to about one million years in a constant density environment. The basic stages of evolution of a ULX Nebula include a non-spherical HII-region with a central cavity created by non-radiative shock waves, an elongated or bipolar shock-powered nebula created by jet activity and a large-scale quasi-spherical bubble.

Keywords: ISM: jets and outflows, ISM: bubbles, stars: individual (SS433), X-rays: individual (ULXs)

1. Introduction

The issue of supercritical accretion is more than three decades old. It was first considered in the seminal paper by Shakura and Sunyaev (1973) who pointed out the significance of Eddington limit for accretion processes. A mass accretion rate exceeding the critical, or Eddington, value leads to

Eddington luminosity limit violation in the framework of standard disc accretion. The disc may become either advective (Abramowicz et al., 1980) or outflow-dominated (see Poutanen et al. (2007) and references therein) if the critical accretion rate is exceeded.

Supercritical accretors are expected to appear among massive black-hole X-ray binaries during thermal and sometimes nuclear-timescale mass transfer (Rappaport et al., 2005). The released power is in excess of $\sim 10^{39} \text{erg s}^{-1}$ (Eddington luminosity for a conventional $10M_{\odot}$ black hole), that makes supercritical accretors in nearby galaxies prospective targets for X-ray, UV and optical observations. In different models, however, the exact observational properties differ. Both outflows and advection (advective discs are geometrically thick) taken apart make sources anisotropic and soften their spectral energy distributions (SED), thereby increasing the contribution of extreme ultraviolet radiation in the overall energy output. That makes supercritical accretors possible energy sources for bright optical nebulae (Katz, 1986; Abolmasov et al., 2009).

SS433 is known as a unique Galactic object in the supercritical accretion regime (Fabrika, 2004). Although its X-ray luminosity is much lower than the expected Eddington luminosity ($\sim 10^{36} \div 10^{37} \text{erg s}^{-1}$, depending on the interstellar absorption value), similar objects observed at low inclinations $\lesssim 20^{\circ}$ are predicted to be objects of high ($\gtrsim 10^{39} \text{erg s}^{-1}$) X-ray luminosity (Katz, 1986; Poutanen et al., 2007). It allows to link SS433 and the still rather dim concept of supercritical accretion with extragalactic Ultraluminous X-ray sources (ULXs) known to have X-ray luminosities $10^{39} \div 10^{40} \text{erg s}^{-1}$. Though not unique in this sense, the supercritical accretion model qualitatively explains most of the observational properties of ULXs, including their environmental and statistical properties (Swartz et al., 2004; Abolmasov et al., 2007b).

This interpretation is indirectly supported by the fact that some ULXs are identified with powerful nebulae (Pakull and Mirioni, 2003) with sizes from about 10 to hundreds of parsecs. The optical properties of these nebulae are very diverse (see Abolmasov et al. (2007b) for review). Some appear large-scale shock-powered bubbles. However, in several cases an Extreme Ultraviolet (EUV) ionisation source is needed to explain the properties of the nebula or some part of it or some particular emission lines. In the case of the large nebular complex MH9/10/11 around HoIX X-1 (Abolmasov and Moiseev, 2008), two regions powered by shocks and EUV radiation are clearly distinguished by kinematics and emission-line spectrum.

SS433 is surrounded by the radionebula W50 (Dubner et al., 1998) known to harbour optical filaments (Zealey et al., 1980; van den Bergh, 1980). Recent spectroscopic results (Boumis et al., 2007; Abolmasov et al., 2010) show that bright [N II] and [O III] emissions are broadened by $\sim 50 \text{ km s}^{-1}$. Their relatively high intensities (in comparison with Balmer emissions) are easy to explain if Galactic abundance gradients are taken into account. The structure of the nebula is seen in details, but it is difficult to infer its integral properties such as total line luminosities and line ratios because of heavy and patchy absorption toward the nebula and its large angular size (about 1 deg). The total emission line spectrum of W50 may differ significantly from the spectra of the bright filaments.

There were several works concerning the evolution of W50 (Zavala et al., 2008; Velázquez and Raga, 2000). They agree about the leading role of the relativistic jets of SS433 in forming the peculiar “seashell” shape of the nebula, but its central round core is usually attributed to the pre-existing supernova remnant that is an essential element of all the models. It is however unclear whether the supernova cavity is required to reproduce the observed morphology. Another complication is the non-relativistic wind of the supercritical disc of SS433 (Fabrika, 2004). Its power is about an order of magnitude less than that of jets, but still sufficient to provide the energy of an average supernova explosion of $\sim 10^{51} \text{ erg}$ in $\sim 10^5 \text{ yr}$ period. Though it is natural to expect the compact object in SS433 to be formed in a supernova explosion, the significance of its contribution to the power of the nebula is uncertain.

Here we make some estimates of the properties that a nebula produced by an SS433-like object should have when evolving in a constant-density environment. We consider two main energy sources: mildly relativistic jets with the kinetic luminosity of $L_j = 2 \times 10^{39} \text{ erg s}^{-1}$ and a photoionizing anisotropic EUV/X-ray radiation source with a polar-angle-dependent SED calculated according to Abolmasov et al. (2009). There are also energy sources like the supernova explosion that was likely to precede the formation of the compact accretor and a slow wind similar to that of SS433 (Fabrika, 2004). Both processes are expected to be much less energetic than the jet activity and photoionizing radiation of the object.

In the next section we consider the basic properties of the HII-region produced by the photoionizing radiation of the central source. In section 3 we present several quasi-2D photoionization models. In section 4 we consider the evolution of a jet-blown (beambag) nebula. We compare the results with

the existing properties of ULXNe and related objects (including W50 and the putative relic ULX bubble in IC10) and discuss our results in section 5.

2. Strömgen Zone

Supercritical accretors are expected to be anisotropic sources due to geometrical and relativistic beaming effects. Both X-ray radiation and some part of the EUV photons (that are most relevant for nebular physics) escape only in the certain range of polar angles forming a complex non-spherical HII-region. We introduce here a generalized version of the Strömgen radius:

$$R_S = \left(\frac{s}{\alpha n_e^2} \right)^{1/3} \simeq 260 n_0^{-2/3} s_{50}^{1/3} \text{pc} \quad (1)$$

Here n_0 is hydrogen density, α is hydrogen recombination coefficient (see for example Osterbrock and Ferland (2006)), $s = dS/d\Omega$ is the number of hydrogen-ionizing quanta emitted in a unit solid angle. s_{50} is s in 10^{50}s^{-1} units. For an isotropic source, R_s is simply the radius of its Strömgen sphere. A strongly anisotropic source produces a bilobial or elongated nebula like the one shown in figure 1.

A quasi-2D sectoral approximation is more than sufficient for order-of-magnitude estimates. Deviations from this approximation are mainly due to re-emission of absorbed ionizing quanta and are therefore $\sim (\alpha_A - \alpha_B)/\alpha_A \sim 0.1$, where $\alpha_{A,B}$ are recombination coefficients for the A and B cases, correspondingly (Osterbrock and Ferland, 2006). Deviations from the sectoral approximation are expected to be of the order 10%. As long as these effects are not very important one may consider the nebula extended by $R_S(\theta)$ in any direction characterised by polar angle θ . In the next section, we calculate the structure of the nebula in more detail but still in a sectoral approximation: at any polar angle θ , the radial structure is calculated as for a spherical nebula using our supercritical accretion disc model spectrum for appropriate inclination angle $i = \theta$.

A Strömgen zone has a characteristic expansion time equal to the recombination time (Dopita and Sutherland, 2003):

$$t_S = 1/\alpha n_e \simeq 1.2 \times 10^5 T_4^{0.85} n_0^{-1} \text{yr} \quad (2)$$

The expansion proceeds roughly according to the law $R(t) \propto (1 - \exp\{-t/t_S\})^{1/3}$. Internal pressure leads to further expansion of the HII-region but the expan-

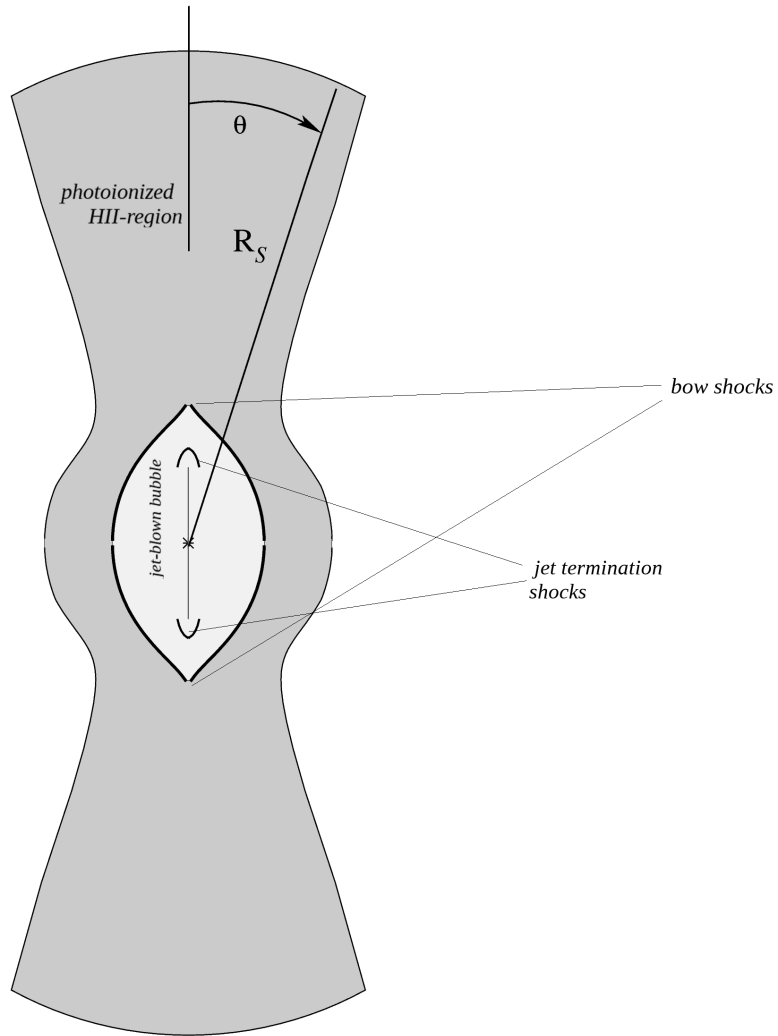


Figure 1: Principal scheme of a hybrid nebula produced by a supercritical accretor. Protruding parts of the nebula are produced by the anisotropic radiation field.

sion velocities are close to the thermal and are therefore overridden by the expanding jet-blown bubbles. We discuss this in more detail in section 4.

We use our model of an outflow-dominated supercritical disc (Abolmasov et al., 2009) to calculate the inclination-dependent spectral energy distribution. It is dominated by X-rays and extreme ultraviolet (EUV) radiation inside the funnel (for polar angles less than the funnel half-opening angle, $\theta_f \sim 20^\circ$) and by UV and optical at larger angles. Extended low-inclination parts of the nebula receive a broad-band ionizing spectrum rich in soft X-rays and in EUV, similar to that of active galactic nuclei (AGN).

X-ray ionized nebulae (XINe) differ from ordinary nebulae powered by EUV radiation in several ways. One is that XINe do not have any sharp outer boundary but the boundary is determined by either absorption of X-rays or the equilibrium temperature. The outer radius of a XIN may be estimated as the radius of penetration of standard or soft X-rays bearing most of the energy.

$$R_X \simeq \frac{1}{n\sigma(E)}, \quad (3)$$

where $\sigma(E)$ is the absorption cross-section at energy $E \sim T \sim 1$ keV below which most of the quanta are emitted. Using the simple approximation of Hayakawa (1973), one arrives to the following estimate:

$$R_X \simeq 1.6T_1^{2.5}n_0^{-1}\text{kpc} \quad (4)$$

T_1 here is the characteristic temperature of the energy source in keV. The electron temperature fades away in XINe in a power-law fashion (roughly as $T \propto r^{-1/2}$, see Rappaport et al. (1994)) therefore the definition of the outer radius of a nebula powered by X-rays is largely uncertain.

3. Quasi-2D Modelling

In order to understand the basic properties of the photoionized nebulae we suggested that the Strömgren zone is established in a quasi-2D way: the structure of the HII-region in every given direction is determined by the generalized quanta production rate only (that is a function of the polar angle). For every polar angle value, a spherical model was calculated. A set of 50 spherical models for polar angles between 0 and $\pi/2$ was calculated. Three series of spherical *Cloudy* (version 08.00) models were computed: one for a low ISM density (1cm^{-3}) and solar metallicity, one for an

Table 1: Integral luminosities (10^{37}ergs^{-1} units) of some selected lines for the three *CLOUDY* models described in section 3.

line ID	1cm^{-3} , solar metallicity	100cm^{-3} , solar metallicity	100cm^{-3} , 0.1 solar metallicity
$\text{H}\beta$	100	106	110
$[\text{O III}]\lambda 5007$	990	1260	320
$[\text{O II}]\lambda 3727$	270	154	60
$[\text{O I}]\lambda 6300$	44	39	13
$\text{He II}\lambda 4686$	38	21	20
$[\text{S II}]\lambda 6717$	28	30	13
$\text{Fe VII}\lambda 6087$	5.1×10^{-3}	8.3×10^{-3}	1.8×10^{-3}
$\text{He I}\lambda 4471$	8.7×10^{-3}	7.1×10^{-3}	7.4×10^{-3}
$[\text{O III}]\lambda 4363$	0.044	0.066	0.037
$[\text{Fe III}]\lambda 4659$	4.3×10^{-3}	2.2×10^{-3}	4.2×10^{-4}

HII-region density of 100cm^{-3} and solar metallicity, and one for the high density of 100cm^{-3} and metallicity ten times less than solar. The inner radius is set to 10pc in order to reproduce the compact inner cavern created by shocks. The input spectrum was calculated using the supercritical funnel model by Abolmasov et al. (2009) with $\dot{m} = 100$, $\theta_f = 0.4\text{rad} \simeq 23^\circ$, $r_{in} = 1/6\dot{m} = 1/600$ and self-irradiation accounted for by two iterations (see original work by Abolmasov et al. (2009) for details).

In figures 2–4, we show the two-dimensional emissivity maps (cross-sections) of the model nebulae using combined sets of *Cloudy* simulations. The scale everywhere is linear. As may be seen in the figures, a nebula usually has two characteristic radii, one corresponding to the Strömberg zone of the disc wind photosphere and the other to the nebula produced by the funnel interior. This structure is well established in recombination lines (see figure 2). The emissivity of a collisionally excited line is high in a narrow layer where the relevant ionic species is abundant and fades smoothly away outside the Strömberg radius where ionization by X-rays is important (see figure 3). Other lines such as $\text{He I}\lambda 4471$ and coronal emissions are sensitive to additional heating (see figure 4).

The luminosities of selected emission lines calculated with the three models are given in table 1. Note the $\text{He II}\lambda 4686$ to $\text{H}\beta$ flux ratios about $0.2\div 0.3$

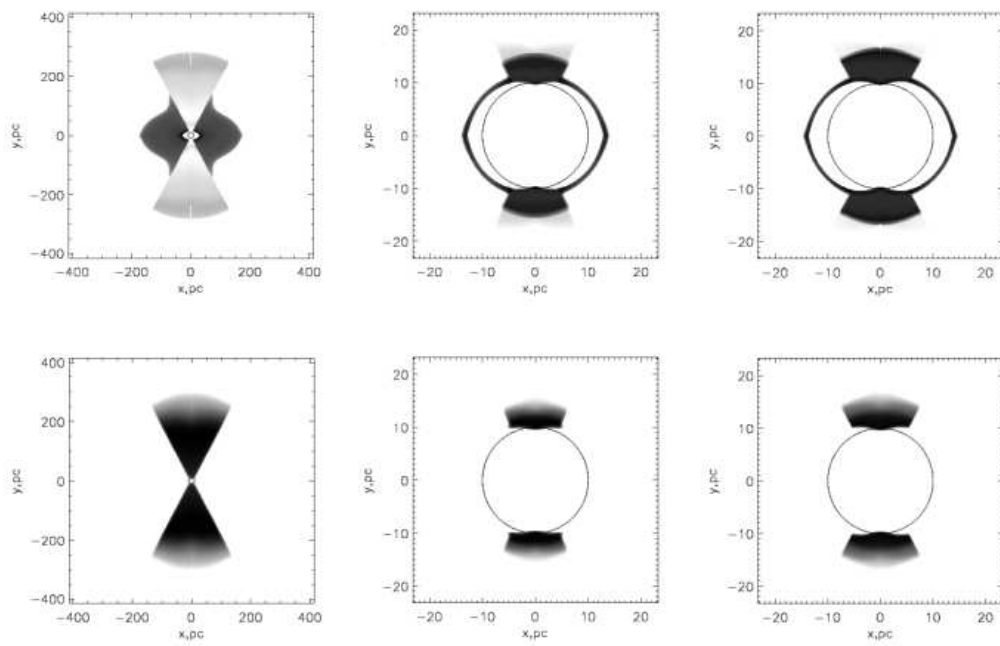


Figure 2: Model emissivities of recombination lines: $H\beta$ (upper row) and $He\ II\ \lambda 4686$ (lower row). From left to right the pictures correspond to the low-density, high-density and low-metallicity models.

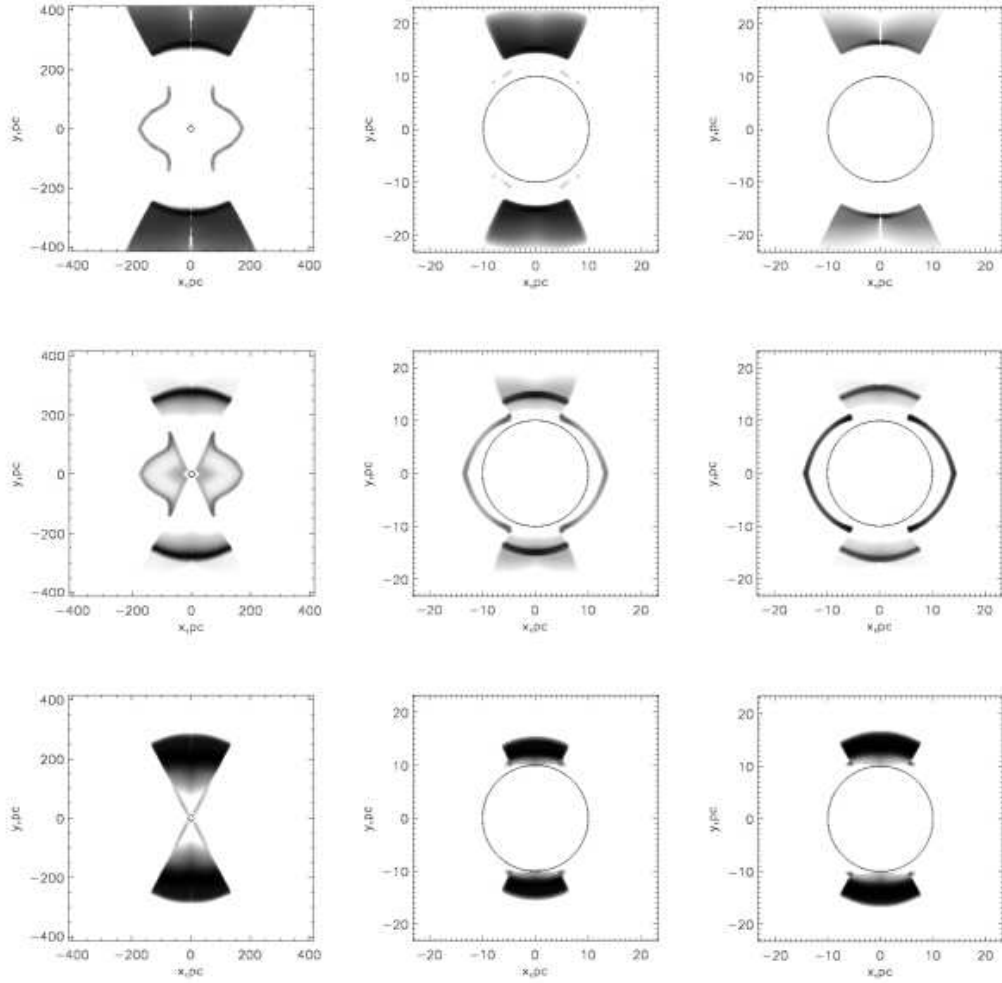


Figure 3: Model emissivities of oxygen lines excited by collisions (from top to bottom): $[\text{O I}]\lambda 6300$, $[\text{O II}]\lambda 3727$ and $[\text{O III}]\lambda 5007$. The models are in the same order.

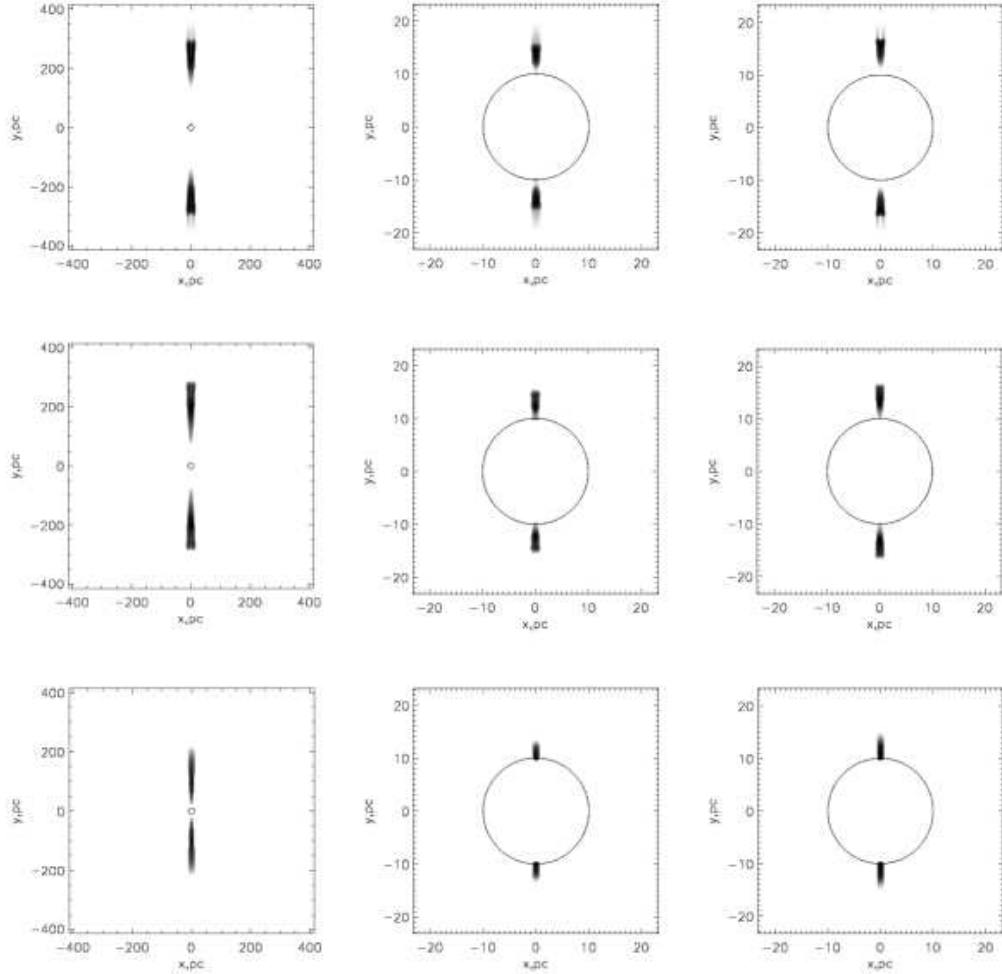


Figure 4: Model emissivities of emission lines sensitive to heating: He I $\lambda 4471$ (upper row), [O III] $\lambda 4363$ (second row) and “coronal” Fe VII $\lambda 6078$ (bottom). The models are in the same order.

and very high [OIII] λ 5007 to $H\beta$ flux ratios around 10 (for higher metallicity). These values together with rather bright collisionally-excited lines of low ionization potentials like [O I] λ 6300 and [S II] λ 6717 are consistent with the spectra of ULX nebulae proposed as HII-regions excited by the hard central radiation source such as the nebula of M101X98 (Abolmasov et al., 2007b) and MH11 (Abolmasov and Moiseev, 2008). The properties of some individual ULX nebulae will be discussed in section 5. It should be also noted that the real nebular spectra are usually obtained with either a slit or a finite-size aperture that distorts the observed spectrum. Luminosities of low-ionization emissions may be underestimated by observational data.

4. Bubble Nebulae

4.1. Jet Propagation Law

The expected evolution of the nebula produced by relativistic jets is similar to the scenario proposed by Begelman and Cioffi (1989) for AGN. Unlike the intergalactic and galactic media in the case of radiogalaxies, the interstellar medium density is more or less constant that prevents ULXs from forming extended shock-powered lobes.

The jet propagation is governed by the momentum balance at the jet head. In the reference system of the bow shock, the ram pressure of the unshocked material plus thermal pressure of the medium should be balanced by the momentum flux in the jet equal to $\beta(\gamma - 1)L_j/2c\Omega_j$ where Ω_j is the solid angle of a single jet. If jets are precessing or jittering, Ω_j effectively will be larger. L_j is the luminosity of the jet pair.

We neglect the pressure of the unshocked jet material. In the case of SS433, the gas pressure is about eight orders of magnitude less than the bulk-motion momentum flux in the region where moving emission lines are formed. If this ratio holds, contribution of the jet gas pressure is always negligible. This statement is even stronger if the gas is a subject to radiative or adiabatic cooling.

$$\rho \left(\frac{dz}{dt} \right)^2 + P = \frac{\beta(\gamma - 1)L_j}{2c\Omega_j z^2} \quad (5)$$

The solution may be found analytically. There is a characteristic time t_j of jet deceleration, and a maximal length of the jet R_j that can not be exceeded. Until R_j is reached, jet head moves according to the law:

$$\zeta = \sqrt{\tau(2 - \tau)}, \quad (6)$$

where ζ and τ are correspondingly the dimensionless jet length and age, $\zeta = z/R_j$ and $\tau = t/t_j$. Final position of the jet head in this approximation equals:

$$R_j \simeq 36 \sqrt{\frac{\Omega_j}{\gamma_j \beta_j}} L_{39}^{1/2} n_0^{-1/2} T_4^{-1/2} \text{ pc} \quad (7)$$

Here, L_{39} , n_0 and T_4 are the jet kinetic luminosity in $10^{39} \text{ erg s}^{-1}$, interstellar medium hydrogen density in cm^{-3} and its temperature in 10^4 K (note that the gas is ionized and heated by the radiation of the central source). The jet head position is stationary for $t > t_j$ because the interstellar pressure P becomes significant.

Characteristic time scale t_j of jet deceleration equals:

$$t_j \simeq 3 \sqrt{\frac{\Omega_j}{\gamma_j \beta_j}} L_{39}^{1/2} n_0^{-1/2} T_4 \text{ Myr} \quad (8)$$

The jet bubble size is the size of a pressure-driven bubble filled with hot gas and expanding according to the well-known law established by Avedisova (1972) (see also Castor et al. (1975) and Lozinskaia (1986)):

$$R_{JB} \simeq 100 L_{39}^{1/5} n_0^{-1/5} t_6^{3/5} \text{ pc}, \quad (9)$$

where t_6 is time in million years (Myr). Radius of a wind-blown bubble may be estimated in the same way. In the case of SS433, the power of the isotropic wind is about one order of magnitude lower.

$$R_{WB} \simeq 70 L_{w,38}^{1/5} n_0^{-1/5} t_6^{3/5} \text{ pc} \quad (10)$$

The characteristic radii as functions of time for fixed ISM density and other parameters are shown in figure 6.

4.2. Line Luminosities

Below we use the luminosities of Balmer lines as characteristic. Two energy sources are expected to produce strong nebular lines: photoionization by

the central X-ray/EUV source and radiative shock waves. One may estimate the contribution of the shock-powered part of the nebula as:

$$L_S(H\beta) = (3.26 \times 10^{-3} V_2^{-0.59} + 4.32 \times 10^{-3} V_2^{-0.72} \Theta(V_2 - 1.5)) L_j, \quad (11)$$

where L_j is the mechanical luminosity of the wind or jets, V_2 is the velocity (in 100 km s^{-1} units) of the shock actually producing the optical emission. Θ here is the Heaviside function, equal to 0 if its argument is less than 0 and 1 otherwise. It is used to switch on the shock wave precursor for velocities higher than about 150 km s^{-1} (Dopita and Sutherland, 1996).

The $H\beta$ luminosity of the HII-region may be estimated as:

$$L_H(H\beta) \simeq 5 \times 10^{37} Q_{50} \text{erg s}^{-1} \quad (12)$$

Q_{50} here is the total production rate of hydrogen-ionizing quanta in 10^{50} s^{-1} units. An EUV source with a luminosity $L_{EUV} \sim 10^{40} \text{ erg s}^{-1}$ provides $Q \sim 4 \times 10^{50} \text{ s}^{-1}$.

Several important details should be mentioned concerning emission line luminosities: *(i)* shock waves should become radiative in order to produce optical nebular emission; *(ii)* shock emission disappears if the velocity is very low, $V_S \lesssim 20 \text{ km s}^{-1}$; *(iii)* a shock wave leaves a cavern of rarefied gas practically transparent to ionizing radiation. Generally, photoionization produces brighter lines but the shape of the nebula is determined by shock waves.

We assume that the primary source of mechanical energy is a pair of jets with a total power $L_j = 2 \times 10^{39} \text{ erg s}^{-1}$ in order to simulate an SS433-like system. Below we will trace the evolution of such a system for several million years. All the jet power is supposed to be distributed over a given solid angle Ω_j due to precession or jitter; we assume $\Omega_j = 0.038 \text{ sr}$. If one considers an SS433-like object with a stationary jet ($\Omega_j \sim 10^{-3} \div 10^{-4}$), R_j becomes much higher, about $1 \div 3 \text{ kpc}$. As far as I am concerned, structures of this kind (kiloparsec-scale double-lobe nebulae) have not ever been observed. ISM density is likely to vary significantly on these spatial scales. In a spiral galaxy, the most likely fate of a kiloparsec-scale jet is leaving the galactic disc and producing a fountain.

Characteristic time scales are: the Strömngren zone establishment time, t_S , the jet propagation time, t_j , the shock cooling (to temperatures when the shocked gas becomes radiative; see for example Castor et al. (1975)) time t_{cool} .

$$t_S \simeq 1 Q_{50}^{1/2} n_0^{-1/2} T_4^{-3/4} \text{Myr} \quad (13)$$

$$t_j \simeq 3 \sqrt{\frac{\Omega_j}{\gamma_j \beta_j}} L_{39}^{1/2} n_0^{-1/2} T_4 \text{ Myr} \quad (14)$$

$$t_{cool} \simeq 3 \times 10^4 L_{39}^{1/2} n_0^{-1/2} \text{ yr} \quad (15)$$

In figures 5-7, we illustrate the dependence of various parameters of the nebula on time and ISM density. Generally, the nebula around a supercritical accretor is powered by photoionization until shock waves become radiative. Its properties are expected to be similar to the model nebulae described in the previous section, but the hot cavern in the center expands with time.

A double bow shock nebula may exist even at longer times but usually jet bubble expansion velocities are higher and the nebula appears to be either a bubble or a multi-bubble shock-powered shell. Bubble coalescence is a poorly constrained process. Under almost any possible conditions, expansion of the two jet-powered bubbles is fast enough to produce a single cocoon at the very moment of jet launching.

4.3. Double Bow Shock and Bubble Stages

The HII-region is torn from inside by the expanding jets and jet bubbles. I consider the nebula in the double bow shock dominated stage if the jet head propagation velocity is higher than the jet bubble expansion velocity. The bubble expansion is expected to be highly anisotropic in the “bow shock” stage but the details are uncertain and depend on the gas flows inside the bubble. I would also expect the morphology of the shell to depend on the ratio of the two velocities. I assume the nebula is in the “double bow shock” stage if the jet propagation velocity is higher than bubble expansion velocity, and in the “single bubble” stage otherwise.

Generally, “double bow shock” nebulae exist in rarefied medium indicating that there should be a correlation between the elongated or bilobial form of the nebula and the low density of the ambient medium. ULXs located inside star-forming regions or molecular clouds are expected to evolve rapidly toward the quasi-isotropic single bubble stage.

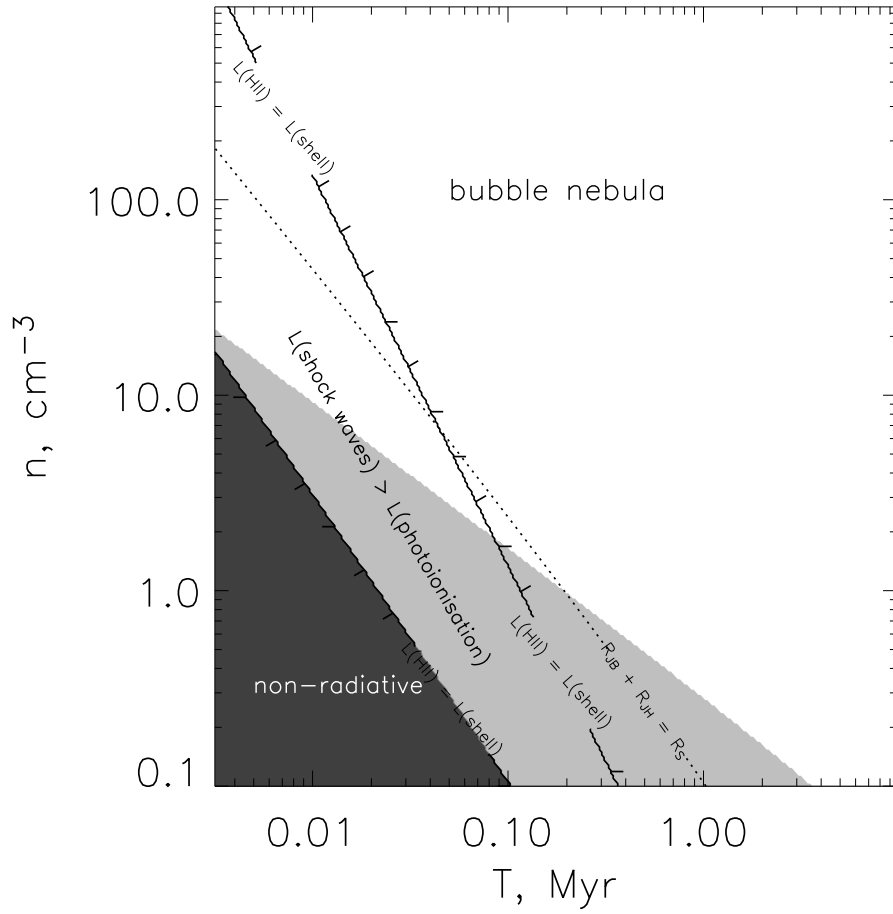


Figure 5: Emission regimes of a nebula powered by a supercritical accretor. Shock waves are non-radiative in shaded regions (in the darkest area, both bow shocks and bubbles are non-radiative). The straight line with ticks demarcates the regions where photoionization and shock waves are expected to dominate the Balmer line emission, respectively. At the dotted line, the sizes of the jet-blown bubble and the Strömgen zone are approximately equal.

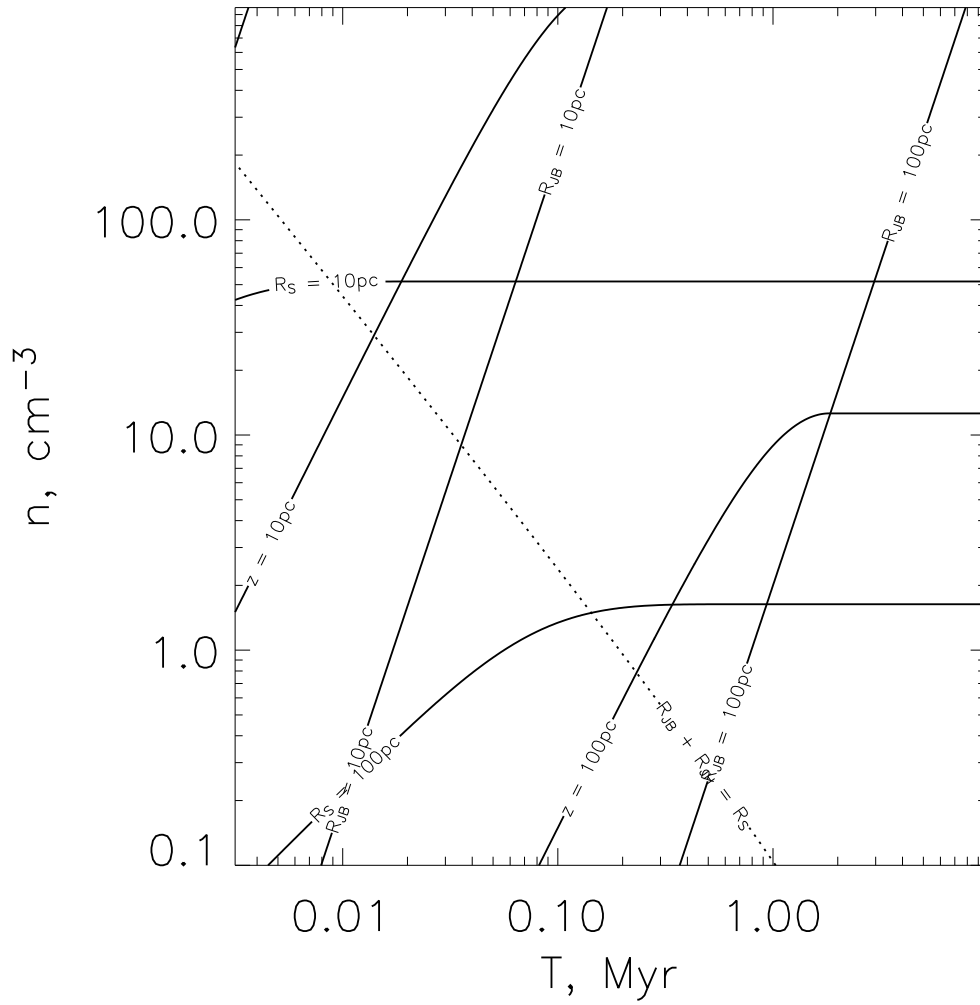


Figure 6: Various characteristic radii as functions of system age and ISM density. R_S , R_{JB} and z are correspondingly the Strömgen radius, jet-blown bubble radius and jet length. See text for details.

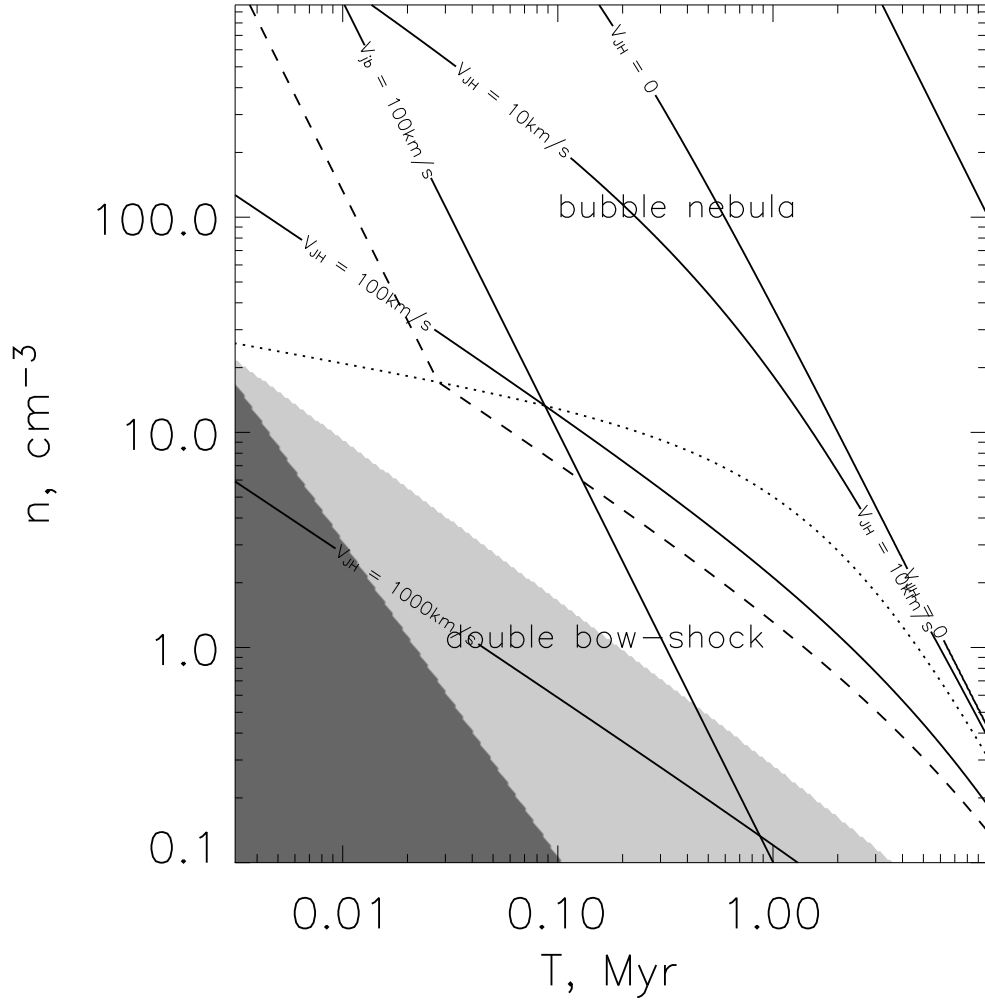


Figure 7: Jet head and jet bubble expansion velocities as functions of the age and ISM density. The dotted line shows the boundary between the double bow shock case (jet propagation velocity is higher than the bubble expansion velocity) and the bubble/multibubble stage. The dashed line demarcates the regions of fast (with precursors) and slow shock waves. In the shaded region, shocks are non-radiative (cooling time is comparable to or higher than the age of the system).

5. Discussion

5.1. Comparison with Observations

The large diversity of the observational properties of ULX nebulae may be explained (at least qualitatively) in the framework of a hybrid model taking into account both EUV radiation and shock waves. Let us see how individual objects fit into this unified scheme.

MF16 is a well-known but outstanding example. It is the most compact of all the known ULXNe and has the highest expansion rate measured ($V \sim 200 \text{ km s}^{-1}$). It was shown to have an elongated bilobial morphology with a fainter extended halo surrounding a prominent shell with a radius of $10 \div 20 \text{ pc}$ (Blair et al., 2001). All these parameters are consistent with the position around $n_0 \sim 5 \text{ cm}^{-3}$, $t \sim 30\,000 \text{ yr}$ in our diagrams. The extended halo probably corresponds to the outer part of the HII-region that is expected to be larger than the jet bubble radius at this age. The ISM density was estimated in Abolmasov et al. (2008) and equals $n_0 \simeq 6 \text{ cm}^{-3}$. The uniqueness of MF16 is probably the result of its evolutionary stage that lasts less than one tenth of the expected lifetime of the source.

Several objects selected by Pakull and Mirioni (2003) are large-scale bubbles with dynamical ages $\sim 1 \text{ Myr}$ and quasi-spherical morphology probably affected by underlying density gradients. It is likely that their expansion started in a rather dense environment of the host star-forming region that implies an effective density value of $n_0 \sim 10 \div 100 \text{ cm}^{-3}$.

Predicted lifetimes for nuclear-timescale accretion in massive X-ray binaries are of the order 1 Myr (Rappaport et al., 2005), which is comparable to the dynamical ages of ULX bubbles. It is possible that the bubble survives the further evolution of the object that is expected to evolve toward a binary system similar to Cyg X-3 or IC10 X-1 (Bauer and Brandt, 2004), consisting of a black hole and a Wolf-Rayet donor. In this scope, the giant synchrotron superbubble around IC10 X-1 (Lozinskaya and Moiseev, 2007) is the best candidate for a relic ULX bubble. Its kinematical properties are close to those of the largest ULX bubble nebulae (Abolmasov, 2008). The concurrent explanation of the bubble in IC10 as a hypernova remnant can not account for this similarity.

HoII X-1 does not show any signatures of supersonic motions or contamination with heavy elements (Lehmann et al., 2005). The nebula appears to be larger than the Strömgren radius inferred from recombination line luminosities (Abolmasov and Moiseev, 2008; Abolmasov et al., 2008) that may be

explained by a non-radiative central cavern created by the preceding supernova explosion and/or wind/jet activity. This is consistent with the observed non-thermal radiospectrum of the nebula.

W50 is also quite easy to place on the diagram. The undisturbed ISM density $\sim 2 \text{ cm}^{-3}$ is known from Lockman et al. (2007) so the nebula may be considered a prototype of an evolved ULXNe in a rarefied environment. Its properties are consistent with an age about several $\times 10^5$ yr and ISM density $\sim 2 \text{ cm}^{-3}$. These estimates imply that the bubble expansion velocity for *W50* should be $V_{JB} \sim 50 \div 100 \text{ km s}^{-1}$ consistent with velocity estimates by Zealey et al. (1980); Boumis et al. (2007); Abolmasov et al. (2010).

5.2. Jet-Powered Nebulae

The ambiguity of the energy sources of ULXNe bears some similarity with the question about the power sources of Seyfert Narrow-Line Regions (NLRs). This similarity is most striking for MF16 (Abolmasov et al., 2007a) where the integral spectrum itself is similar to that of a Seyfert NLR.

Another parallel with AGN is in the pair of relativistic jets that in the case of SS433-like objects are likely to produce something similar to the cocoons that were predicted (Begelman and Cioffi, 1989) but are not observed around AGN mainly due to strong gradients in ISM and IGM density.

Little can be said for certain about the structure of a nebula produced by relativistic jets. However, *W50*, ULXNe and similar objects are prospective targets for sophisticated hydrodynamical modeling. For example, in the works by Velázquez and Raga (2000) and Zavala et al. (2008), hydrodynamical simulations allowed to qualitatively explain the basic properties of *W50*. I suggest that running simulations at slightly different parameters would allow to better understand the diversity of ULXNe that sometimes evolve into quasi-spherical bubbles, but under different conditions may retain a resemblance to *W50* instead (as in the case of MF16).

6. Conclusions

In this article, I have shown that most of the observational properties of ULX nebulae may be explained by a single unified scheme. Only two free parameters were varied (ISM density and the age of the source), though some divergence in the parameters of the binary system itself is expected.

One of the main results is the bipolar morphology in some “hot” lines such as He II λ 4686 and [O III] emissions. The “ionization cone” structures

detected by Roberts et al. (2003) and the elongated high-excitation nebulae around M101P098 and HoIX X-1 are naturally explained in the framework of our model. Bilobial and elongated shock-powered nebulae are expected to appear in a low-density environment due to the different dependences of the jet propagation and bubble expansion velocities on the ambient density. The morphology of ULX shells is predicted to evolve through a “double bow shock” bipolar structure toward a quasi-isotropic single bubble stage.

Supercritical accretors are likely to exist for about 1Myr (of the order of the nuclear timescale of the donor star). Then the source is expected to evolve into a WR+BH binary, possibly surrounded by a relic ULX bubble. We propose that the synchrotron bubble in IC10 is a relic ULX bubble rather than a hypernova remnant.

References

- Abolmasov, P., 2008. Ultraluminous X-ray Sources and Their Nebulae, in: M. Axelsson (Ed.), American Institute of Physics Conference Series, pp. 33–38.
- Abolmasov, P., Fabrika, S., Sholukhova, O., Afanasiev, V., 2007a. Integral Field Spectroscopy of a Peculiar Supernova Remnant MF16 in NGC6946, in: Kissler-Patig, M., Walsh, J.R., Roth, M.M. (Eds.), Science Perspectives for 3D Spectroscopy, pp. 327–+.
- Abolmasov, P., Fabrika, S., Sholukhova, O., Afanasiev, V., 2007b. Spectroscopy of optical counterparts of ultraluminous X-ray sources. *Astrophysical Bulletin* 62, 36–51. [arXiv:astro-ph/0612765](#).
- Abolmasov, P., Fabrika, S., Sholukhova, O., Kotani, T., 2008. Optical Spectroscopy of the ULX-Associated Nebula MF16. *ArXiv e-prints* 0809.0409.
- Abolmasov, P., Karpov, S., Kotani, T., 2009. Optically Thick Outflows of Supercritical Accretion Discs: Radiative Diffusion Approach. *PASJ* 61, 213–. 0809.0917.
- Abolmasov, P., Maryeva, O., Burenkov, A.N., 2010. The Eastern filament of W50. *Astronomische Nachrichten* 331, 412–+. 1003.4706.
- Abolmasov, P., Moiseev, A.V., 2008. Kinematics of the Nebular Complex MH9/10/11 Associated with HoIX X-1. *Revista Mexicana de Astronomia y Astrofisica* 44, 301–309. 0806.4527.

- Abramowicz, M.A., Calvani, M., Nobili, L., 1980. Thick accretion disks with super-Eddington luminosities. *ApJ* 242, 772–788.
- Avedisova, V.S., 1972. Formation of Nebulae by Wolf-Rayet Stars. *Soviet Astronomy* 15, 708–+.
- Bauer, F.E., Brandt, W.N., 2004. Chandra and Hubble Space Telescope Confirmation of the Luminous and Variable X-Ray Source IC 10 X-1 as a Possible Wolf-Rayet, Black Hole Binary. *ApJL* 601, L67–L70. [arXiv:astro-ph/0310039](#).
- Begelman, M.C., Cioffi, D.F., 1989. Overpressured cocoons in extragalactic radio sources. *ApJL* 345, L21–L24.
- Blair, W.P., Fesen, R.A., Schlegel, E.M., 2001. Hubble Space Telescope Images of the Ultraluminous Supernova Remnant Complex in NGC 6946. *AJ* 121, 1497–1506.
- Boumis, P., Meaburn, J., Alikakos, J., Redman, M.P., Akras, S., Mavromatakis, F., López, J.A., Caulet, A., Goudis, C.D., 2007. Deep optical observations of the interaction of the SS 433 microquasar jet with the W50 radio continuum shell. *MNRAS* 381, 308–318. [arXiv:0707.4243](#).
- Castor, J., McCray, R., Weaver, R., 1975. Interstellar bubbles. *ApJL* 200, L107–L110.
- Dopita, M.A., Sutherland, R.S., 1996. Spectral Signatures of Fast Shocks. I. Low-Density Model Grid. *ApJSS* 102, 161–+.
- Dopita, M.A., Sutherland, R.S., 2003. Astrophysics of the diffuse universe. *Astrophysics of the diffuse universe*, Berlin, New York: Springer, 2003. Astronomy and astrophysics library, ISBN 3540433627.
- Dubner, G.M., Holdaway, M., Goss, W.M., Mirabel, I.F., 1998. A High-Resolution Radio Study of the W50-SS 433 System and the Surrounding Medium. *AJ* 116, 1842–1855.
- Fabrika, S., 2004. The jets and supercritical accretion disk in SS433. *Astrophysics and Space Physics Reviews* 12, 1–152. [arXiv:astro-ph/0603390](#).
- Hayakawa, S., 1973. Circumstellar Matter in the Accretion Model of Cosmic X-Ray Sources. *Progress of Theoretical Physics* 50, 459–471.

- Katz, J.I., 1986. SS433 - Another view. *Comments on Astrophysics* 11, 201–211.
- Lehmann, I., Becker, T., Fabrika, S., Roth, M., Miyaji, T., Afanasiev, V., Sholukhova, O., Sánchez, S.F., Greiner, J., Hasinger, G., Costantini, E., Surkov, A., Burenkov, A., 2005. Integral field spectroscopy of the ultraluminous X-ray source Holmberg II X-1. *A&A* 431, 847–860. [arXiv:astro-ph/0410458](#).
- Lockman, F.J., Blundell, K.M., Goss, W.M., 2007. The distance to SS433/W50 and its interaction with the interstellar medium. *MNRAS* 381, 881–893. [arXiv:0707.0506](#).
- Lozinskaia, T.A., 1986. *Sverkhnovyye zvezdy i zvezdnyi veter : vzaimodeistvie S gazom Galaktiki*. Moskva : "Nauka," Glav. red. fiziko-matematicheskoi lit-ry, 1986.
- Lozinskaya, T.A., Moiseev, A.V., 2007. A synchrotron superbubble in the IC10 galaxy: a hypernova remnant? *MNRAS* 381, L26–L29. [arXiv:0708.0626](#).
- Osterbrock, D.E., Ferland, G.J., 2006. *Astrophysics of gaseous nebulae and active galactic nuclei*.
- Pakull, M.W., Mirioni, L., 2003. Bubble Nebulae around Ultraluminous X-Ray Sources, in: Arthur, J., Henney, W.J. (Eds.), *Revista Mexicana de Astronomia y Astrofisica Conference Series*, pp. 197–199.
- Poutanen, J., Lipunova, G., Fabrika, S., Butkevich, A.G., Abolmasov, P., 2007. Supercritically accreting stellar mass black holes as ultraluminous X-ray sources. *MNRAS* 377, 1187–1194. [arXiv:astro-ph/0609274](#).
- Rappaport, S., Chiang, E., Kallman, T., Malina, R., 1994. Ionization nebulae surrounding supersoft X-ray sources. *ApJ* 431, 237–246.
- Rappaport, S., Podsiadlowski, P., Pfahl, E., 2005. Stellar-Mass Black Hole Binaries as ULXs, in: L. Burderi, L. A. Antonelli, F. D’Antona, T. di Salvo, G. L. Israel, L. Piersanti, A. Tornambè, & O. Straniero (Ed.), *Interacting Binaries: Accretion, Evolution, and Outcomes*, pp. 422–433.

- Roberts, T.P., Goad, M.R., Ward, M.J., Warwick, R.S., 2003. The unusual supernova remnant surrounding the ultraluminous X-ray source IC 342 X-1. *MNRAS* 342, 709–714. [arXiv:astro-ph/0303110](#).
- Shakura, N.I., Sunyaev, R.A., 1973. Black holes in binary systems. Observational appearance. *A&A* 24, 337–355.
- Swartz, D.A., Ghosh, K.K., Tennant, A.F., Wu, K., 2004. The Ultraluminous X-Ray Source Population from the Chandra Archive of Galaxies. *ApJSS* 154, 519–539. [arXiv:astro-ph/0405498](#).
- van den Bergh, S., 1980. The Optical Remnant of W50 = SS433. *ApJL* 236, L23+.
- Velázquez, P.F., Raga, A.C., 2000. A numerical simulation of the W 50-SS 433 system. *A&A* 362, 780–785.
- Zavala, J., Velázquez, P.F., Cerqueira, A.H., Dubner, G.M., 2008. 3D hydrodynamical simulations of the large scale structure of W50-SS433. *ArXiv e-prints* 804.0804.0491.
- Zealey, W.J., Dopita, M.A., Malin, D.F., 1980. The interaction between the relativistic jets of SS433 and the interstellar medium. *MNRAS* 192, 731–743.